A new MOF-5 homologue for selective separation of methane from C_2 hydrocarbons at room temperature

Yabing He,[1,a] Chengling Song,[1] Yajing Ling,[1] Chuande Wu,[2] Rajamani Krishna,[3] and Banglin Chen[4,5,b]
[1]*College of Chemistry and Life Sciences, Zhejiang Normal University, Jinhua 321004, China*
[2]*Department of Chemistry, Zhejiang University, Hangzhou 310027, China*
[3]*Van't Hoff Institute for Molecular Sciences, University of Amsterdam, Science Park 904, 1098 XH Amsterdam, The Netherlands*
[4]*Department of Chemistry, University of Texas at San Antonio, One UTSA Circle, San Antonio, Texas 78249-0698, USA*
[5]*Department of Chemistry, Faculty of Science, King Abdulaziz University, Jeddah 22254, Saudi Arabia*

(Received 11 July 2014; accepted 12 August 2014; published online 13 October 2014)

A new MOF-5 homologue compound **UTSA-10** has been obtained under solvothermal conditions from a mixture of $Zn(NO_3)_2 \cdot 6H_2O$ and commercially available linker, 2-methylfumaric acid, in *N*,*N*-dimethylformamide. The moderate surface area and suitable pore sizes enable the activated **UTSA-10a** to separate methane from C_2 hydrocarbons at room temperature. [http://dx.doi.org/10.1063/1.4897351]

Metal-organic frameworks (MOFs) are a new type of functional porous materials consisting of metal ions or metal containing clusters connected by multidentate organic linkers via metal coordination bonds. By bridging metal ions/clusters with organic linkers, a plethora of compounds with different pore sizes, properties, and functionalities can be systematically designed and synthesized. Compared to conventional porous materials such as zeolites and activated carbons, these hybrid materials have high surface areas and pore volumes, uniform pore sizes, and chemical functionalities. Moreover, their pore sizes and chemical functionalities can be tuned by modifying the metal groups or organic linkers. Hence, MOFs have attracted considerable interest, which has been fueled by the promise of their utilities in gas sorption, separation, heterogeneous catalysis, sensing, and biomedicine.[1–11]

Nature gas, one of the most important energy resources, mainly consists of methane and also contains small quantities of other hydrocarbons heavier than methane. The removal of these hydrocarbons from natural gas is traditionally carried out by cryogenic distillation, which is very energy-intensive. In contrast, selective adsorption separation near room temperature using porous materials offers an energy-efficient alternative. A few MOF materials have been reported to show the potential for the selective separation of C_2/C_1 hydrocarbons,[12–17] but the research in this respect is still somewhat limited to date.

MOF-5 ($Zn_4O(BDC)_3$, BDC = 1,4-benzenedicarboxylate) is a prototypical MOF consisting of a cubic framework built from Zn_4O clusters connected via benzenedicarboxylates.[18] Due to the large surface area, exceptional pore volume, and relatively high thermal stability, it has been widely studied in a variety of fields and usually considered to be a benchmark MOF. Yaghi *et al.* employed isoreticular synthesis method to prepare a series of **MOF-5** homologues with identical topology but diverse porosity and different chemical functionalization.[19] One member of this series exhibited a high capacity for methane storage. Xue *et al.* used a fumaric acid to construct

[a]E-mail: heyabing@zjnu.cn
[b]E-mail: banglin.chen@utsa.edu. Fax: +1-210-458-7428.

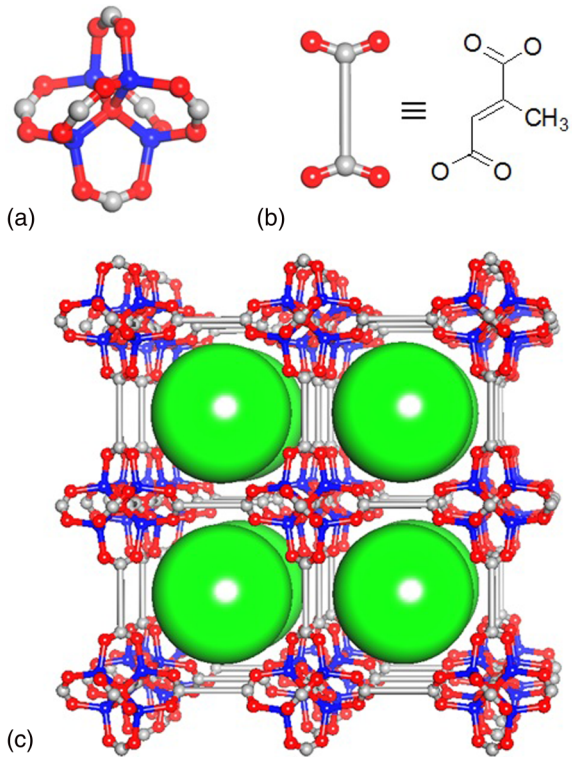

FIG. 1. Schematic representation of the structure of **UTSA-10a** with a cubic framework (c) built from Zn_4O clusters (a) connected via 2-methylformarate (b).

another **MOF-5** homologue ($Zn_4O(FMA)_3$, FMA = fumarate) exhibiting moderate gas sorption due to comparatively low surface area.[20] Herein, we report another prototypical MOF-5 homologue, **UTSA-10**, which is assembled from a readily available dicarboxylate, namely, 2-methylfumarate, in expectation that the methyl group in the organic linker improves the moisture stability and tunes the pore size of the resulting MOF for gas separation application. The activated **UTSA-10a** shows a good potential for the separation of methane from C_2 hydrocarbons at room temperature, which has been comprehensively established by gas sorption isotherms and transient breakthrough and pulse chromatographic simulations.

UTSA-10 was readily synthesized by a solvothermal reaction of 2-methylfumaric acid and $Zn(NO_3)_2 \cdot 6H_2O$ in *N*,*N*-dimethylformamide (DMF) at 100 °C for 48 h as colorless cubic crystals. The crystal structure was revealed by the similarity of its powder X-ray diffraction (PXRD) pattern to the simulated one from a MOF $[Zn_4O(FMA)_3]$[20] that is built from the fumarate ligand of the same length as 2-methylfumarate.[21] **UTSA-10** adopts a cubic framework structure by connecting $Zn_4O(COO)_6$ clusters with the 2-methylfumarate linkers (Fig. 1). The presence of methyl groups did not interfere with the formation of the isoreticular structure. **UTSA-10** can be formulated as $[Zn_4O(MeFMA)_3] \cdot 8DMF \cdot 2H_2O$ (MeFMA = 2-methylfumarate) on the basis of thermal gravimetric analysis (TGA, supplementary Fig. S1[22]) and microanalysis. TGA under a nitrogen atmosphere shows that the desolvated MOF is thermally stable up to 360 °C.

The permanent porosity was unambiguously established by the N_2 sorption isotherm at 77 K. Prior to gas sorption measurement, the as-synthesized **UTSA-10** was guest-exchanged with dry acetone and evacuated under a dynamic vacuum at room temperature for 24 h to generate the activated **UTSA-10a**. Its PXRD pattern matches with that of the pristine sample (supplementary Fig. S2[22]), indicating that the structure remains intact after activation. The N_2 sorption isotherm at 77 K shows a characteristic type-I adsorption behavior (Fig. 2), which is typical for microporous materials. **UTSA-10a** can adsorb 282 cm^3 (STP) g^{-1} of N_2 at 77 K. Based on the N_2 adsorption isotherms, the Brunauer-Emmett-Teller (BET) and Langmuir surface areas are calculated to be 1090

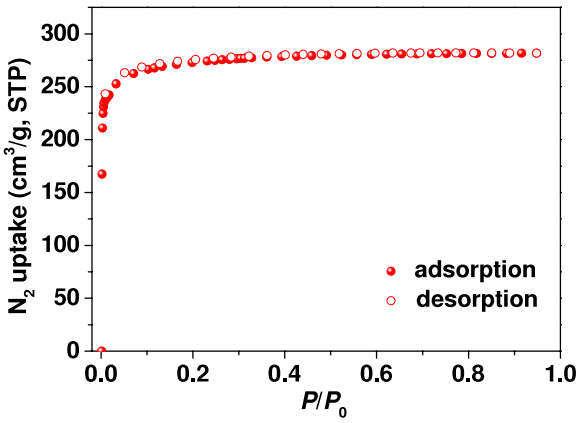

FIG. 2. N_2 sorption isotherm of **UTSA-10a** at 77 K. The solid and open symbols represent the adsorption and desorption data, respectively. STP = Standard Temperature and Pressure.

and 1146 $m^2\ g^{-1}$, respectively (supplementary Figs. S3 and S4[22]). The total pore volume calculated from the maximum amount of N_2 adsorbed is 0.4358 $cm^3\ g^{-1}$. These values are smaller than those of **MOF-5**[18] and $[Zn_4O(FMA)_3]$[20] materials.

We have recently paid much attention to porous MOFs for the storage and separation of small hydrocarbons because of their very important industrial applications.[12,13,23–30] Given the fact the pore size within **UTSA-10a** tuned by the methyl group in the organic linker falls in the range of the kinetic diameters of C_1 and C_2 hydrocarbons (3.3–4.4 Å), the low-pressure single-component C_2H_2, C_2H_4, C_2H_6, and CH_4 adsorption properties were examined accordingly at two different temperatures of 273 and 296 K. As shown in Fig. 3, all isotherms, except the C_2H_2 one, show good reversible sorption behavior. At 296 K and 1 atm, **UTSA-10a** takes up a negligible amount of CH_4 (5.8 $cm^3\ g^{-1}$), but a moderate amount of C_2H_2 (43.0 $cm^3\ g^{-1}$), C_2H_4 (31.0 $cm^3\ g^{-1}$), and C_2H_6 (48.5 $cm^3\ g^{-1}$). The uptakes of C_2 hydrocarbons are higher than those of **MOF-5**[31] despite a lower surface area. The higher C_2 hydrocarbon adsorption capacities in comparison with methane indicate that **UTSA-10a** is a very attractive material for the selective adsorptive separation of C_2 hydrocarbons from methane at room temperature.

Based on the pure-component gas sorption isotherms, the Henry's law and IAST (Ideal Adsorbed Solution Theory) selectivities were calculated. The Henry's law selectivities for C_2H_2, C_2H_4, and C_2H_6 over CH_4 at 296 K are 8.1, 4.6, and 6.5, respectively, which are moderate compared to those of the best performing MOF materials.[13] Furthermore, IAST has been applied to calculate adsorption selectivities for an equimolar quaternary $CH_4/C_2H_2/C_2H_4/C_2H_6$ gas mixture in **UTSA-10a** as a function of the total bulk gas phase pressure at 296 K. It was observed from

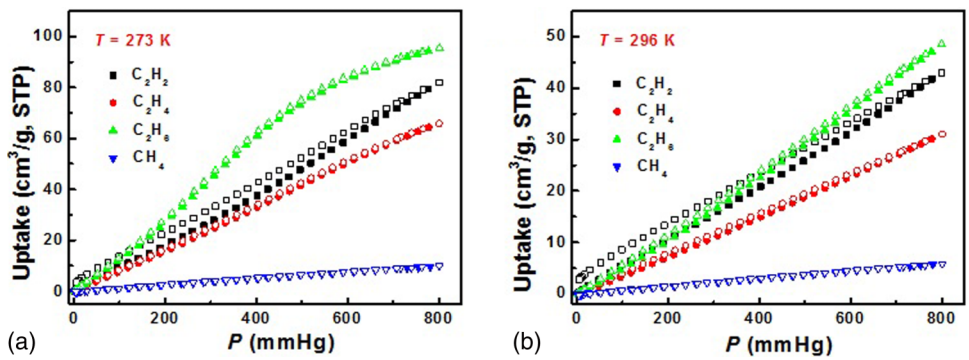

FIG. 3. The single-component C_2H_2, C_2H_4, C_2H_6, and CH_4 sorption isotherms of **UTSA-10a** at 273 K (a) and 296 K (b). The solid and open symbols represent the adsorption and desorption data, respectively.

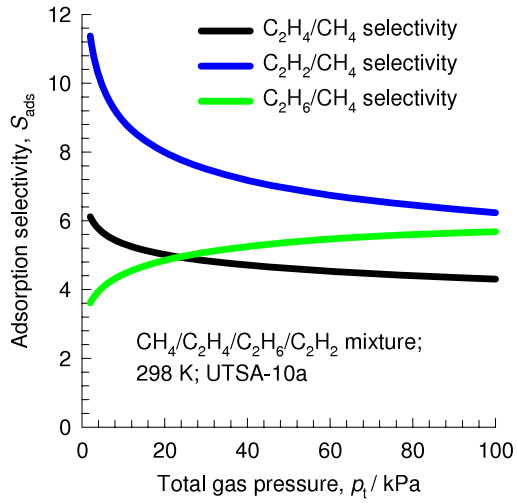

FIG. 4. Calculations using IAST of Myers and Prausnitz[32] for C_2H_2/CH_4, C_2H_4/CH_4, and C_2H_6/CH_4 selectivities for an equimolar quaternary $CH_4/C_2H_2/C_2H_4/C_2H_6$ gas mixture maintained at isothermal conditions at 296 K using **UTSA-10a**.

Fig. 4 that C_2H_2/CH_4 and C_2H_4/CH_4 selectivities decrease, while C_2H_6/CH_4 adsorption selectivities increase, with increasing pressure. The adsorption selectivities of C_2 hydrocarbons with respect to CH_4 fall in the range of 4–12; this indicates that it is possible to use **UTSA-10a** for selective adsorption of C_2 hydrocarbons from CH_4.

To understand the separation selectivity, the isosteric enthalpies of adsorption was calculated using the Clausius-Clapeyron equation by fitting the pure-component adsorption isotherms at 273 K and 296 K to a Langmuir-Freundlich expression (supplementary Fig. S5[22]). Fig. 5 presents the isosteric enthalpies of adsorption for C_2H_2, C_2H_4, C_2H_6, and CH_4 in **UTSA-10a** as a function of component loadings. Interestingly, the isosteric enthalpies keep constant, independent of surface coverage. The isosteric enthalpy of adsorption of methane is significantly lower and has a value of 13.2 kJ mol^{-1}, whereas the isosteric enthalpy of adsorption of C_2 hydrocarbons has a value of about 19–27 kJ mol^{-1}. Thus, the preferable adsorption of C_2 hydrocarbons relative to C_1 methane is attributed to the stronger interaction of the framework with C_2 hydrocarbons. Moreover, compared

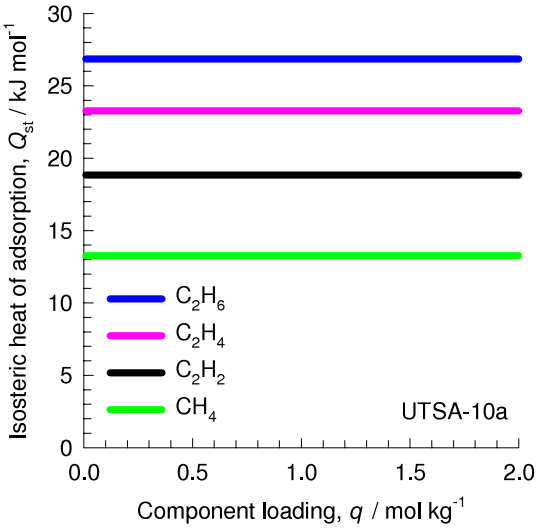

FIG. 5. Comparison of the heats of adsorption of C_2H_6, C_2H_4, C_2H_2, and CH_4 in **UTSA-10a**.

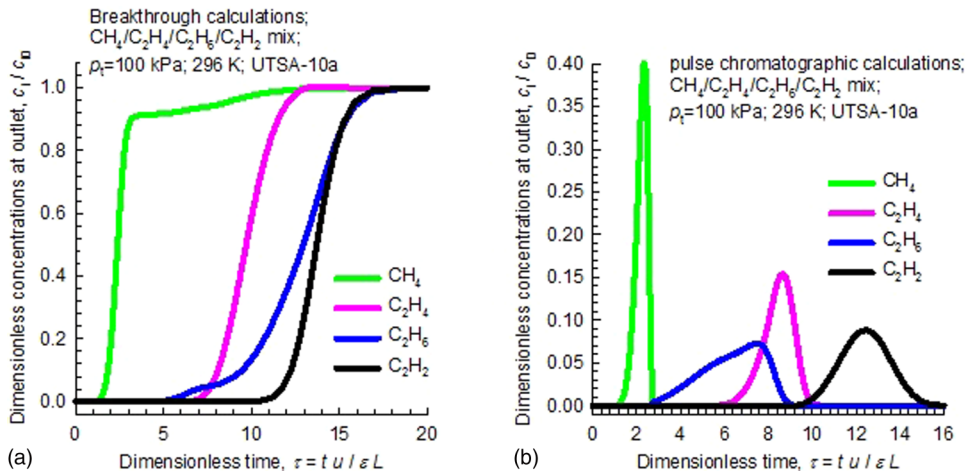

FIG. 6. (a) Breakthrough characteristics of an adsorber packed with **UTSA-10a** maintained at isothermal conditions at 296 K. The inlet gas is an equimolar 4-component quaternary $CH_4/C_2H_2/C_2H_4/C_2H_6$ gas mixture maintained at isothermal conditions at 296 K and 100 kPa, with partial pressures for each component of 25 kPa. Video animations showing the motion of gas phase concentration fronts traversing the length of the adsorber with an equimolar 4-component $CH_4/C_2H_2/C_2H_4/C_2H_6$ mixture have been provided as the supplementary material. (b) Pulse chromatographic simulations of an adsorber packed with **UTSA-10a** and maintained at isothermal conditions at 296 K. At the inlet to the adsorber, a pulse of an equimolar 4-component quaternary $CH_4/C_2H_2/C_2H_4/C_2H_6$ gas mixture is injected for a duration of 10 s.

to the best-performing materials, the low isosteric enthalpy of adsorption indicates the low regeneration cost. It should be pointed out that an ideal adsorbent for gas separation should possess low regeneration cost, besides high uptake capacity and high adsorption selectivity, which need to be equally taken into consideration.

To further demonstrate the separation feasibility, we carried out transient breakthrough and pulse chromatographic simulations following the methodologies of Krishna and Long.[13,15,24,33,34] The details are provided in the supplementary material. As shown in Fig. 6(a), for an equimolar 4-component gas mixture of C_2H_2, C_2H_4, C_2H_6, and CH_4 maintained at isothermal conditions at 296 K and a total pressure of 100 kPa at the inlet of the adsorber packed with **UTSA-10a**, the sequence of breakthroughs is CH_4, C_2H_6, C_2H_4, and C_2H_2. There is a significant time interval between the breakthrough of CH_4 and C_2 hydrocarbons. Therefore, it is possible to recover pure methane from this 4-component mixture during the adsorption cycle (see video animations provided in the supplementary material). Fig. 6(b) presents the pulse chromatographic separation of an equimolar 4-component CH_4–C_2H_2–C_2H_4–C_2H_6 mixture with **UTSA-10a** at 296 K. The first peak to emerge from the adsorber is that of methane which can be recovered in nearly pure form. The next sets of peaks are for the C_2 hydrocarbons. Taken together, these simulated data clearly suggest that **UTSA-10a** can effectively separate methane from C_2 hydrocarbons.

In summary, we used a commercially available dicarboxylate to synthesize a new **MOF-5** homologue material, namely, **UTSA-10a**. Gas sorption isotherm measurements and simulated breakthrough studies have comprehensively demonstrated that the MOF has a good potential for the separation of methane from C_2 hydrocarbons at ambient temperature.

This work was supported by an AX-1730 grant from Welch Foundation (BC), the National Natural Science foundation of China (No. 21301156), Open Research Fund of Top Key Discipline of Chemistry in Zhejiang Provincial Colleges, and Key Laboratory of the Ministry of Education for Advanced Catalysis Materials (Zhejiang Normal University, ZJHX201313).

[1] Y. Cui, Y. Yue, G. Qian, and B. Chen, Chem. Rev. **112**, 1126–1162 (2012).
[2] Y. He, W. Zhou, G. Qian, and B. Chen, Chem. Soc. Rev. **43**, 5657–5678 (2014).
[3] P. Horcajada, R. Gref, T. Baati, P. K. Allan, G. Maurin, P. Couvreur, G. Férey, R. E. Morris, and C. Serre, Chem. Rev. **112**, 1232–1268 (2012).

[4] J.-R. Li, J. Sculley, and H.-C. Zhou, Chem. Rev. **112**, 869–932 (2012).
[5] L. E. Kreno, K. Leong, O. K. Farha, M. Allendorf, R. P. V. Duyne, and J. T. Hupp, Chem. Rev. **112**, 1105–1125 (2012).
[6] H. Wu, Q. Gong, D. H. Olson, and J. Li, Chem. Rev. **112**, 836–868 (2012).
[7] S. Kitagawa, R. Kitaura, and S.-i. Noro, Angew. Chem., Int. Ed. **43**, 2334–2375 (2004).
[8] M. P. Suh, H. J. Park, T. K. Prasad, and D.-W. Lim, Chem. Rev. **112**, 782–835 (2012).
[9] H.-L. Jiang and Q. Xu, Chem. Commun. **47**, 3351–3370 (2011).
[10] L. Ma, C. Abney, and W. Lin, Chem. Soc. Rev. **38**, 1248–1256 (2009).
[11] Y. Liu, W. Xuan, and Y. Cui, Adv. Mater. **22**, 4112–4135 (2010).
[12] M. C. Das, H. Xu, S. Xiang, Z. Zhang, H. D. Arman, G. Qian, and B. Chen, Chem. - Eur. J. **17**, 7817–7822 (2011).
[13] Y. He, R. Krishna, and B. Chen, Energy Environ. Sci. **5**, 9107–9120 (2012).
[14] S. Horike, Y. Inubushi, T. Hori, T. Fukushima, and S. Kitagawa, Chem. Sci. **3**, 116–120 (2012).
[15] E. D. Bloch, W. L. Queen, R. Krishna, J. M. Zadrozny, C. M. Brown, and J. R. Long, Science **335**, 1606–1610 (2012).
[16] J. Cai, J. Yu, H. Xu, Y. He, X. Duan, Y. Cui, C. Wu, B. Chen, and G. Qian, Cryst. Growth Des. **13**, 2094–2097 (2013).
[17] J. Jia, L. Wang, F. Sun, X. Jing, Z. Bian, L. Gao, R. Krishna, and G. Zhu, Chem. - Eur. J. **20**, 9073–9080 (2014).
[18] H. Li, M. Eddaoudi, M. O'Keeffe, and O. M. Yaghi, Nature **402**, 276–279 (1999).
[19] M. Eddaoudi, J. Kim, N. Rosi, D. Vodak, J. Wachter, M. O'Keeffe, and O. M. Yaghi, Science **295**, 469–472 (2002).
[20] M. Xue, Y. Liu, R. M. Schaffino, S. Xiang, X. Zhao, G.-S. Zhu, S.-L. Qiu, and B. Chen, Inorg. Chem. **48**, 4649–4651 (2009).
[21] Single-crystal X-ray crystallographic data: $Fm\bar{3}m$, $a = b = c = 21.643$ Å, $\alpha = \beta = \gamma = 90°$, $V = 10138$ Å^3.
[22] See supplementary material at http://dx.doi.org/10.1063/1.4897351 for thermal gravimetric analysis; powder X-ray diffraction patterns before and after activation; the BET and Langmuir analysis of N_2 adsorption isotherms; and the Langmuir-Freundlich fits of the gas adsorption isotherms.
[23] Y. He, W. Zhou, R. Krishna, and B. Chen, Chem. Commun. **48**, 11813–11831 (2012).
[24] Y. He, S. Xiang, Z. Zhang, S. Xiong, F. R. Fronczek, R. Krishna, M. O'Keeffee, and B. Chen, Chem. Commun. **48**, 10856–10858 (2012).
[25] Y. He, Z. Zhang, S. Xiang, F. R. Fronczek, R. Krishna, and B. Chen, Chem. Commun. **48**, 6493–6495 (2012).
[26] Y. He, Z. Zhang, S. Xiang, F. R. Fronczek, R. Krishna, and B. Chen, Chem. - Eur. J. **18**, 613–619 (2012).
[27] Y. He, Z. Zhang, S. Xiang, H. Wu, F. R. Fronczek, W. Zhou, R. Krishna, M. O'Keeffe, and B. Chen, Chem. - Eur. J. **18**, 1901–1904 (2012).
[28] S. Xiang, Z. Zhang, C.-G. Zhao, K. Hong, X. Zhao, D.-L. Ding, M.-H. Xie, C.-D. Wu, R. Gill, K. M. Thomas, and B. Chen, Nature Commun. **2**, 204 (2012).
[29] H. Xu, Y. He, Z. Zhang, S. Xiang, J. Cai, Y. Cui, Y. Yang, G. Qian, and B. Chen, J. Mater. Chem. A **1**, 77–81 (2013).
[30] M. C. Das, Q. Guo, Y. He, J. Kim, J. C.-G. Zhao, K. Hong, S. Xiang, Z. Zhang, K. M. Thomas, R. Krishna, and B. Chen, J. Am. Chem. Soc. **134**, 8703–8710 (2012).
[31] S. Xiang, W. Zhou, J. M. Gallegos, Y. Liu, and B. Chen, J. Am. Chem. Soc. **131**, 12415–12419 (2009).
[32] A. L. Myers and J. M. Prausnitz, AIChE J. **11**, 121–127 (1965).
[33] R. Krishna and J. R. Long, J. Phys. Chem. C **115**, 12941–12950 (2011).
[34] H. Wu, K. Yao, Y. Zhu, B. Li, Z. Shi, R. Krishna, and J. Li, J. Phys. Chem. C **116**, 16609–16618 (2012).

Supporting Information for the manuscript

A new MOF-5 homologue for selective separation of methane from C_2 hydrocarbons at room temperature

Yabing He*,[a] Chengling Song[a], Yajing Ling[a], Chuande Wu,[b] Rajamani Krishna,[c] and Banglin Chen[d]*

[a] College of Chemistry and Life Sciences, Zhejiang Normal University, Jinhua 321004, China

[b] Department of Chemistry, Zhejiang University, Hangzhou 310027, China

[c] Van 't Hoff Institute for Molecular Sciences, University of Amsterdam, Science Park 904, 1098 XH Amsterdam, The Netherlands

[d] Department of Chemistry, University of Texas at San Antonio, One UTSA Circle, San Antonio, Texas 78249-0698, USA. Fax: (+1)-210-458-7428; E-mail: banglin.chen@utsa.edu

General remarks

All starting materials and reagents for synthesis were commercially available and used as received. Fourier transform infrared (FTIR) spectra were recorded using a Bruke Vector 22 spectrometer between 650 cm^{-1} and 4000 cm^{-1}. Thermogravimetric analyses (TGA) were carried out using a Shimadzu TGA-50 thermal analyzer with a heating rate of 3 ^oC min^{-1} in a flowing nitrogen atmosphere (10 mL min^{-1}). Powder X-ray diffraction (PXRD) patterns were recorded on a Rigaku Ultima IV X-ray diffractometer operating at 40 kV and 44 mA with a scan rate of 1.0 deg min^{-1}, using Cu-K_α radiation. The elemental analyses were performed with Perkin–Elmer 240 CHN analyzers from Galbraith Laboratories, Knoxville. The crystal data were collected on an Oxford Xcalibur Gemini Ultra diffractometer with an Atlas detector. The data were collected using graphite-monochromatic enhanced ultra Cu radiation (λ = 1.54178 Å) at 293 K. A Micromeritics ASAP 2020 surface area analyzer was used to measure gas adsorption isotherms. To have a guest–free framework, the fresh sample was guest–exchanged with dry acetone at least 10 times, filtered and vacuumed at room temperature until the outgas rate was 5 μmHg min^{-1} prior to measurements. A sample of 62.6 mg was used for the sorption measurements and was maintained at 77 K with liquid nitrogen, and at 273 K with an ice–water bath. As the center–controlled air conditioner was set up at 23 ^oC, a water bath was used for adsorption isotherms at 296 K.

Synthesis of UTSA-10

2-methylfumaric acid (H_2MeFMA, 10.0 mg, 76.8 μmol, Aldrich) and $Zn(NO_3)_2 \cdot 6H_2O$ (20 mg, 67.2 μmol, Aldrich) were dissolved in *N*,*N*-dimethylformamide (DMF) (2.0 mL). The mixture was sealed in a screw cap vial and heated at 100 ^oC for 2 days. Colorless crystals were collected in 56% yield. **UTSA-10** can be formulated as $[Zn_4O(MeFMA)_3] \cdot 8DMF \cdot 2H_2O$ on the basis of TGA and microanalysis. TGA data: calcd. weight loss for 8DMF and $2H_2O$: 48.4%, found: 44.1%; Anal. calcd. for $C_{39}H_{72}N_8O_{23}Zn_4$ (%): C, 29.00; H, 3.97; N, 5.34. Found: C, 28.97; H, 4.02; N, 5.42; FTIR (neat, cm^{-1}): 1647, 1583, 1363, 1090, 800.

Fitting of pure component isotherms for UTSA-10a

The experimentally measured loadings of CH_4, C_2H_2, C_2H_4, and C_2H_6, obtained at temperatures at 273 K, and 296 K for **UTSA-10a** were fitted with the Langmuir-Freundlich model

$$q = q_{sat} \frac{bp^{\nu}}{1 + bp^{\nu}} \tag{1}$$

with *T*-dependent parameter *b*

$$b = b_0 \exp\left(\frac{E}{RT}\right) \tag{2}$$

The Langmuir-Freundlich fit parameters are listed in *Table S1*.

Figure S5 provides a comparison of the component loadings of CH_4, C_2H_2, C_2H_4, and C_2H_6, obtained at temperature at 296 K with the Langmuir-Freundlich fits using the parameter sets presented in *Table S1*. The fits are of excellent accuracy over the entire range of pressure.

Isosteric heat of adsorption

The binding energies are reflected in the isosteric heat of adsorption, Q_{st}, defined as

$$Q_{st} = RT^2 \left(\frac{\partial \ln p}{\partial T}\right)_q \tag{3}$$

These calculations are based on the Clausius-Clapeyron equation.

IAST calculations of adsorption selectivity

The selectivity of preferential adsorption of component 1 over component 2 in a mixture containing 1 and 2, perhaps in the presence of other components too, can be formally defined as

$$S_{ads} = \frac{q_1/q_2}{p_1/p_2} \tag{4}$$

In equation (4), q_1 and q_2 are the absolute component loadings of the adsorbed phase in the mixture. The calculations of S_{ads} are based on the use of the Ideal Adsorbed Solution Theory (IAST) of Myers and Prausnitz.[1]

Packed bed adsorber breakthrough simulations

The separation of C_2/C_1 hydrocarbon mixtures is normally carried out within industry using fixed bed adsorbers. The performance of fixed bed adsorbers is dictated by both *adsorption selectivity* and *uptake capacity*. In order to demonstrate the potential of **UTSA-10a** for separation of C_1/C_2 mixtures, we carried out simulations of transient breakthroughs of an equimolar 4-component quaternary $CH_4/C_2H_2/C_2H_4/C_2H_6$ gas mixture maintained at isothermal conditions at 296 K and 100 kPa, with partial pressures for each component of 25 kPa. The methodology used for the breakthrough simulations is the same as described in earlier works.[2,3] Experimental validation of the breakthrough simulation methodology is available in the published literature.[3-8]

For the breakthrough simulations, the following parameter values were used: framework density, ρ = 867 kg m^{-3}; length of packed bed, L = 0.12 m; voidage of packed bed, ε = 0.75; superficial gas velocity at inlet, u = 0.00225 m s^{-1}. The transient breakthrough simulation results are presented in terms of a dimensionless time, τ, defined by dividing the actual time, t, by the characteristic time, $\frac{L\varepsilon}{u}$. Two types of simulations were performed: (a) step input of an equimolar gas mixture, and (b) pulse injection of a gas mixture for a time interval of 10 s.

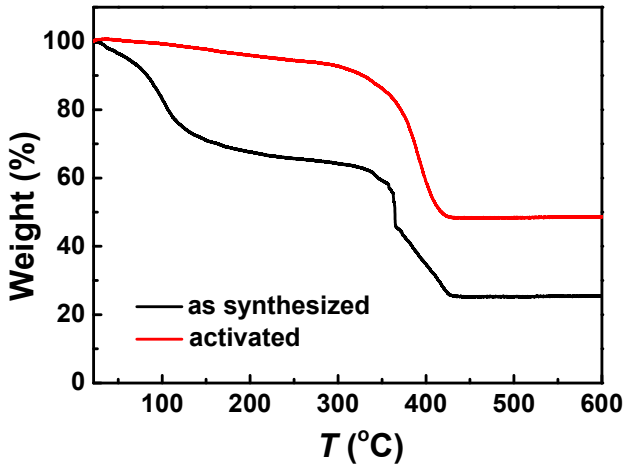

Figure S1. TGA curves of as-sythesized **UTSA-10** (black) and activated **UTSA-10a** (red).

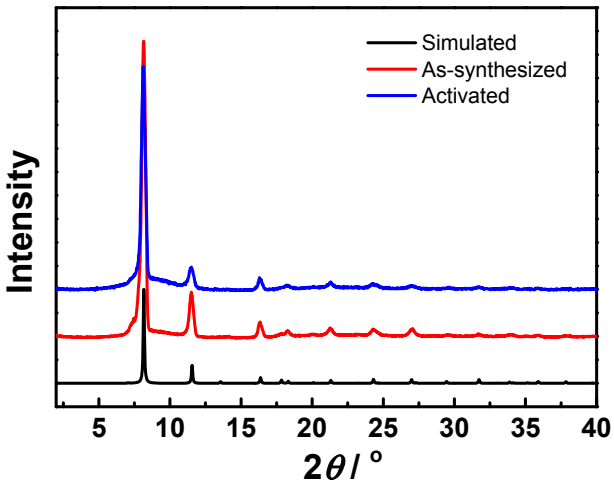

Figure S2. PXRD patterns of the as-synthesized **UTSA-10** (red) and the activated **UTSA-10a** (blue), along with the one simulated from the cif file of $[Zn_4O(FMA)_3]$ (black).

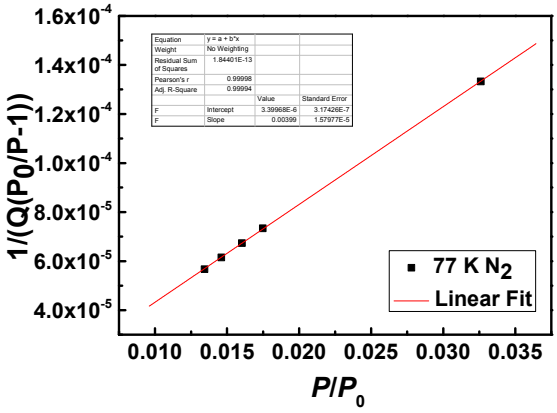

Figure S3. BET analysis of the N_2 adsorption isotherm at 77 K.

S_{BET} = 1/(0.00399 + 3.39968E-6)/22414×6.023×10^{23}×0.162×10^{-18} = 1090 m^2 g^{-1}

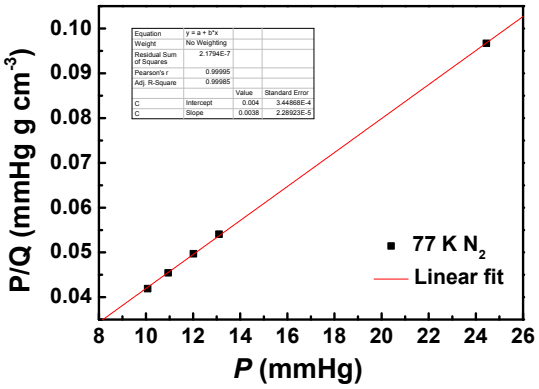

Figure S4. Langmuir analysis of the N_2 adsorption isotherm at 77 K.

$S_{Langmuir}$ = (1/0.0038)/22414×6.023×10^{23}×0.162×10^{-18} = 1146 m^2/g

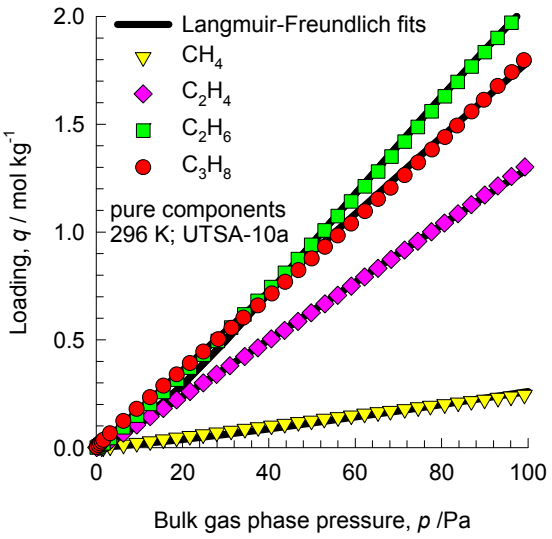

Figure S5. Comparison of the component loadings of CH_4, C_2H_2, C_2H_4, and C_2H_6, obtained at temperatures at 296 K for **UTSA-10a** with the Langmuir-Freundlich fits using the parameter sets presented in *Table S1*.

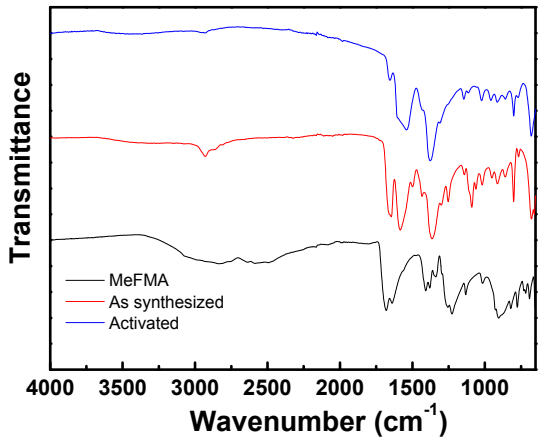

Figure S6. FTIR spectra of the organic ligand (black), as-synthesized **UTSA-10** (red) and activated **UTSA-10a** (blue).

Table S1. Langmuir-Freundlich parameters.

Adsorbate	q_{sat} mol kg^{-1}	b_0 Pa$^{-\nu}$	E kJ mol^{-1}	□ dimensionless
CH_4	30	1.37×10^{-11}	15.9	1.2
C_2H_4	15	9.07×10^{-12}	25.6	1.1
C_2H_6	7.2	9.24×10^{-15}	37.6	1.4
C_2H_2	30	1.69×10^{-10}	19.4	1.03

Reference

1. Myers, A. L.; Prausnitz, J. M. Thermodynamics of mixed gas adsorption, *A.I.Ch.E.J.* **1965**, *11*, 121-130.
2. Krishna, R.; Long, J. R. Screening metal-organic frameworks by analysis of transient breakthrough of gas mixtures in a fixed bed adsorber, *J. Phys. Chem. C* **2011**, *115*, 12941-12950.
3. Krishna, R. The Maxwell-Stefan Description of Mixture Diffusion in Nanoporous Crystalline Materials, *Microporous Mesoporous Mater.* **2014**, *185*, 30-50.
4. Bloch, E. D.; Queen, W. L.; Krishna, R.; Zadrozny, J. M.; Brown, C. M.; Long, J. R. Hydrocarbon Separations in a Metal-Organic Framework with Open Iron(II) Coordination Sites, *Science* **2012**, *335*, 1606-1610.
5. Wu, H.; Yao, K.; Zhu, Y.; Li, B.; Shi, Z.; Krishna, R.; Li, J. Cu-TDPAT, an *rht*-type Dual-Functional Metal–Organic Framework Offering Significant Potential for Use in H_2 and Natural Gas Purification Processes Operating at High Pressures, *J. Phys. Chem. C* **2012**, *116*, 16609-16618.
6. He, Y.; Krishna, R.; Chen, B. Metal-Organic Frameworks with Potential for Energy-Efficient Adsorptive Separation of Light Hydrocarbons, *Energy Environ. Sci.* **2012**, *5*, 9107-9120.
7. Herm, Z. R.; Wiers, B. M.; Van Baten, J. M.; Hudson, M. R.; Zajdel, P.; Brown, C. M.; Maschiocchi, N.; Krishna, R.; Long, J. R. Separation of Hexane Isomers in a Metal-Organic Framework with Triangular Channels, *Science* **2013**, *340*, 960-964.
8. Yang, J.; Krishna, R.; Li, J.; Li, J. Experiments and Simulations on Separating a CO_2/CH_4 Mixture using K-KFI at Low and High Pressures, *Microporous Mesoporous Mater.* **2014**, *184*, 21-27.